2026
doi:10.1017/S1431927622007863
Microsc. Microanal. 28 (Suppl 1), 2022

Infrared Plasmons in Single La-doped $BaSnO_3$ Nanocrystals Revealed by Monochromated STEM-EELS

Hongbin Yang[1], Andrea Konečná[2,3], F. Javier García de Abajo[3,4] and Philip E. Batson[5]

[1.] Department of Chemistry and Chemical Biology, Rutgers University, Piscataway, NJ, USA.
[2.] Central European Institute of Technology, Brno University of Technology, Brno, Czech Republic.
[3.] ICFO - Institute of Photonic Sciences, Castelldefels (Barcelona), Spain.
[4.] ICREA-Institució Catalana de Recerca i Estudis Avançats, Barcelona, Spain.
[5.] Department of Physics and Astronomy, Rutgers University, Piscataway, New Jersey, USA.

Conducting oxides with tunable carrier density and high carrier mobility are emerging as ideal infrared plasmonic materials. In particular, La-doped $BaSnO_3$ (BLSO) has the highest carrier mobility among all perovskite oxides. It is thus a promising alternative to traditional plasmonic materials. Despite the ideal transport and optical properties, high-quality infrared plasmons in this material have yet to be directly observed. Electron energy-loss spectroscopy (EELS) performed in a scanning transmission electron microscope (STEM) has been widely used for probing surface plasmons with high spatial resolution [1]. With the recent improvement in energy resolution [2], infrared plasmons in conducting oxides [3, 4] and metal nanostructures [5, 6] have also been studied in greater detail.

Using a monochromated STEM-EELS, here we demonstrate the existence of low-loss, tunable infrared plasmons in La-doped $BaSnO_3$ [7]. We systematically investigate the dispersion, confinement ratio, and damping of infrared localized surface plasmons (LSPs) in BLSO. Nanocrystals of BLSO are synthesized via a sol-gel method. With 5% La-doping, the screened bulk plasma frequency is found to be around 700 meV, which supports surface plasmons that we observe in the range of 50 – 600 meV. Figure 1 (a) and (b) show EELS energy-filtered maps and spectra of dipolar LSPs for BLSO nanorods with varying dimensions. We observe that both the energy and the spectral width of the LSPs depend strongly on the nanorod length and aspect ratio. From EELS energy-filtered maps, we extract the plasmon wavelength at their resonance energies. As shown in Fig. 1 (c) and (d), these infrared LSPs display a high degree of spatial confinement in comparison to a silver waveguide with similar dimensions. The quality factors (defined as the ratio of the plasmon-energy to the full width at half maximum, FHWM) of these relatively long-lived plasmons are comparable or even better than infrared plasmons in other conducting oxides or metals.

Numerical calculations are also performed to better understand the plasmon damping in BLSO, especially its dependence on nanorod size (Fig. 2). With different nanorod aspect ratio and cross section, we find that the calculated FWHM of the dipolar plasmons changes only slightly around the bulk damping value in the Drude model. From the calculated optical scattering and absorption spectra near BLSO nanorods, we also find that non-radiative damping is the dominant loss mechanism. Thus, surface scattering is likely responsible for the aspect ratio dependence of the FWHM plotted in Fig. 2 for LSPs. Nevertheless, we remark that Fig. 2 demonstrates how narrow infrared plasmons can be realized in BLSO particles of a much smaller sizes than those in noble metals [5, 6].

In summary, low-loss infrared plasmons have been directly observed in La-doped $BaSnO_3$ nanoparticles, where they exhibit much higher confinement ratios the those in noble metals. Our results support La-doped $BaSnO_3$ as a promising alternative to more traditional infrared plasmonic materials [8].

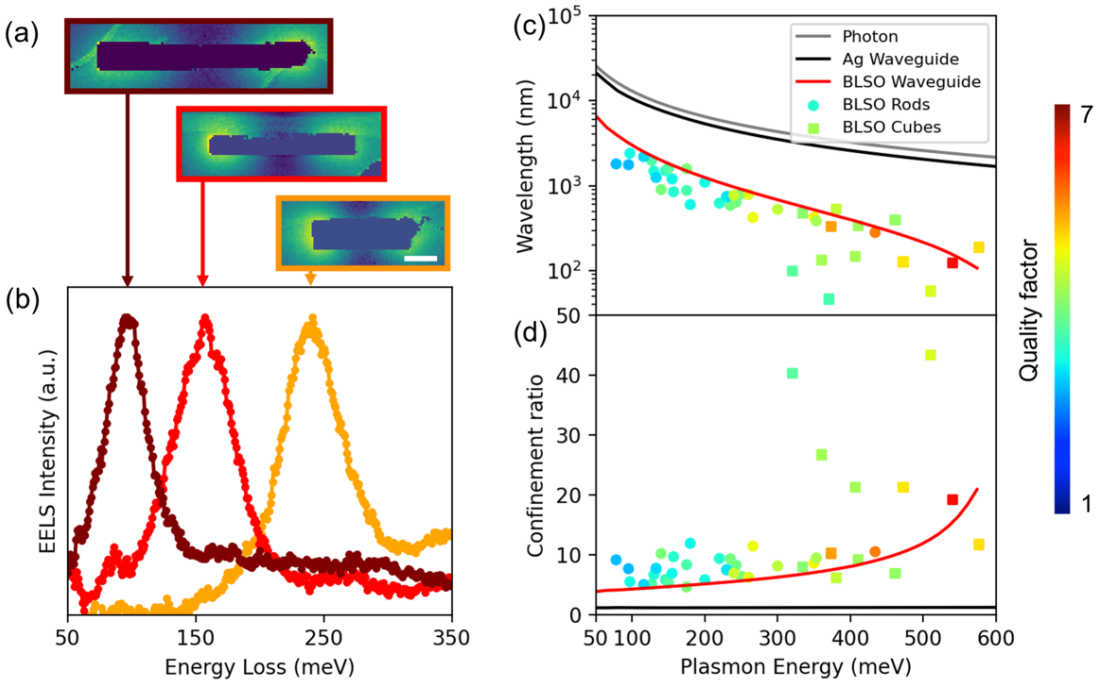

Figure 1. (a) EELS energy-filtered maps of dipolar surface plasmons in BLSO nanorods with varying aspect ratio. The scalebar indicates 100 nm. (b) Aloof electron energy-loss spectra taken near the tips of the three nanorods in (a). (c) Infrared plasmon wavelengths and (d) confinement ratio as a function of plasmon energy measured for BLSO nanoparticles (symbols), as well as BLSO and Ag waveguides (red and black curves). The free-space photon dispersion (gray curve) is shown for reference.

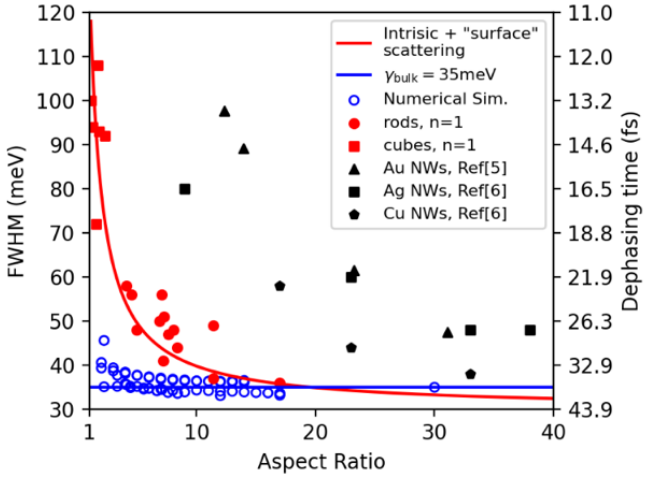

Figure 2. Dependence of the dipolar plasmon FWHM on BLSO nanorod aspect ratio. FWHM of dipolar LSPs measured for BLSO nanorods and cubes (filled red circles and squares) are compared with numerical simulations for particles with similar lateral dimensions but varying cross sections (blue open circles). Results from literature for noble metal nanorods[5, 6] (black) are shown for comparison.

https://doi.org/10.1017/S1431927622007863 Published online by Cambridge University Press

References:

[1] C. Colliex, M. Kociak and O. Stéphan, Ultramicroscopy **162**, A1-A24 (2016).
[2] M. J. Lagos, I. C. Bicket, S. S. Mousavi M and G. A. Botton, Microscopy **71**, i174-i199 (2022).
[3] S. H. Cho, S. Ghosh, Z. J. Berkson, J. A. Hachtel, J. Shi, X. Zhao, L. C. Reimnitz, C. J. Dahlman, Y. Ho, A. Yang, Y. Liu, J.-C. Idrobo, B. F. Chmelka and D. J. Milliron, Chemistry of Materials **31** (7), 2661-2676 (2019).
[4] H. Yang, E. L. Garfunkel and P. E. Batson, Phys. Rev. B **102** (20), 205427 (2020).
[5] Y. Wu, Z. Hu, X.-T. Kong, J. C. Idrobo, A. G. Nixon, P. D. Rack, D. J. Masiello and J. P. Camden, Phys. Rev. B **101** (8) (2020).
[6] V. Mkhitaryan, K. March, E. N. Tseng, X. Li, L. Scarabelli, L. M. Liz-Marzán, S.-Y. Chen, L. H. G. Tizei, O. Stéphan, J.-M. Song, M. Kociak, F. J. García de Abajo and A. Gloter, Nano Lett. **21** (6), 2444-2452 (2021).
[7] H. Yang, A. Konečná, X. Xu, S.-W. Cheong, E. Garfunkel, F. J. García de Abajo and P. E. Batson, arXiv:2111.04144 [physics.app-ph] (2021).
[8] H.Y. and P.E.B. acknowledge the financial support of the US Department of Energy, Office of Science, Basic Energy Sciences under award number DE-SC0005132. F.J.G.A. acknowledges support from the European Research Council (789104-eNANO) and the Spanish MINECO (PID2020-112625GB-I00 and CEX2019-000910-S).